Line Diagnostics: Density, IV

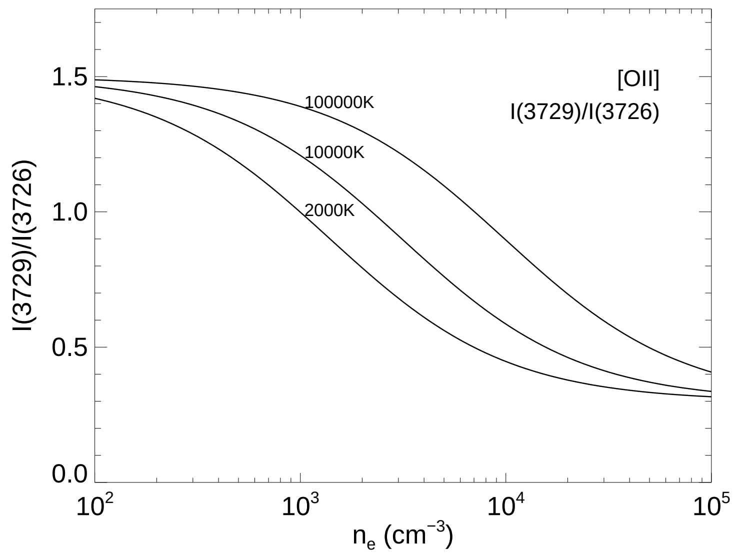

Note: Typical temperatures in AGN are $\sim 10^4$ K

Line Diagnostics: Density, V

Critical densities for $T = 10^4$ K used in AGN work (Hamann et al., 2002; Peterson, 1997).

Transition	n_{cr} (cm^{-3})
[Ne III] λ3869	9.7×10^6
[Ne V] λ3426	1.60×10^7
C II] λ2326	3.16×10^9
C III λ977	1.59×10^{16}
C III] λ1909	1.03×10^{10}
C IV λ1549	2.06×10^{15}
[N I] λ5199	2×10^3
N II] λ2142	9.57×10^9
[N II] λ6548	8.7×10^4
[N II] λ6583	8.7×10^4
N III λ991	8.09×10^{15}
N III] λ1750	1.92×10^{10}
N IV] λ1486	5.07×10^{10}
N V λ1240	3.47×10^{15}

Transition	n_{cr} (cm^{-3})
[O II] λ3727	4.5×10^3
O III λ834	2.14×10^{16}
[O III] λ4363	3.3×10^7
[O III] λ4959	7.0×10^5
[O III] λ5007	7.0×10^5
O III] λ1664	3.13×10^{10}
O IV λ789	1.17×10^{16}
O IV] λ1401	1.12×10^{11}
O VI λ1034	5.53×10^{15}
Si III] λ1892	3.12×10^{11}

Line Diagnostics: Temperature

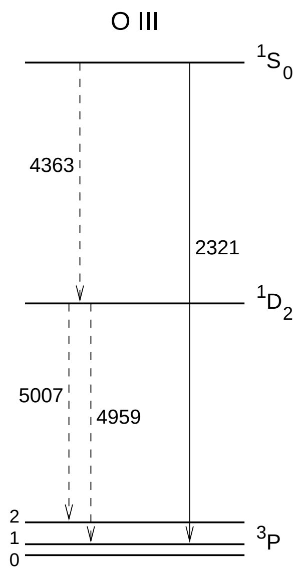

To obtain temperature use two levels with different excitation energy and make use of different collisional excitation probabilities for levels at different energies.

For $T \sim 10000$ K, mainly O III and N II

Line Diagnostics: Temperature

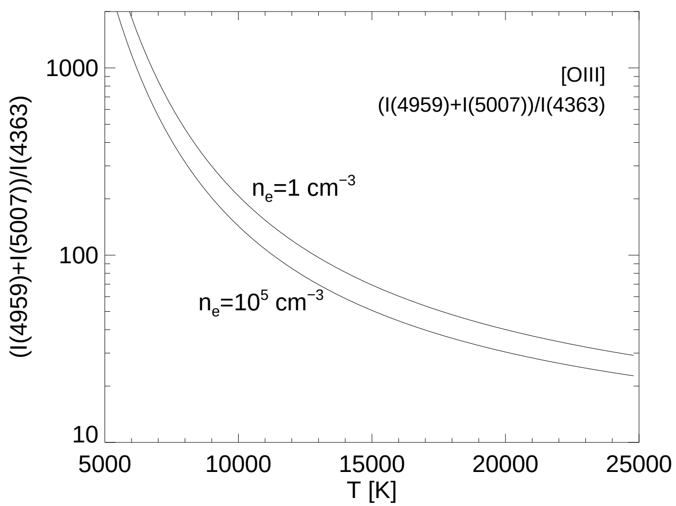

$$\frac{I(4959+5007)}{4363} = \frac{7.7\exp(3.29\times 10^4/T)}{1+4.5\times 10^{-4} n_e T^{-1/2}}$$

Arnaud, M., & Rothenflug, R., 1985, A&AS, 60, 425

Ferland, G. J., & Mushotzky, R. F., 1982, ApJ, 262, 564

Francis, P. J., Hewett, P. C., Foltz, C. B., Chaffee, F. H., Weymann, R. J., & Morris, S. L., 1991, ApJ, 373, 465

Hamann, F., & Ferland, G., 1999, ARA&A, 37, 487

Hamann, F., Korista, K. T., Ferland, G. J., Warner, C., & Baldwin, J., 2002, ApJ, 564, 592

Karzas, W. J., & Latter, R., 1961, ApJS, 6, 167

Korista, K. T., & Ferland, G. J., 1989, ApJ, 343, 678

Mathews, W. G., & Ferland, G. J., 1987, ApJ, 323, 456

Menzel, D. H., & Pekeris, C. L., 1935, MNRAS, 96, 77

Nahar, S. N., Pradhan, A. K., & Zhang, H. L., 2001, ApJS, 133, 255

Osterbrock, D. E., 1989, Astrophysics of gaseous nebulae and active galactic nuclei, (Mill Valley, CA: University Science Books)

Peterson, B. M., 1997, An Introduction to Active Galactic Nuclei, (Cambridge: Cambridge Univ. Press)

Seaton, M. J., 1958, Rev. Mod. Phys., 30, 979

Shull, J. M., & Van Steenburg, M., 1982, ApJS, 48, 95

Verner, D. A., Ferland, G. J., Korista, K. T., & Yakovlev, D. G., 1996, ApJ, 465, 487

Verner, D. A., & Yakovlev, D. G., 1995, A&AS, 109, 125

Wilms, J., Allen, A., & McCray, R., 2000, ApJ, 542, 914

Broad Line Region

Introduction

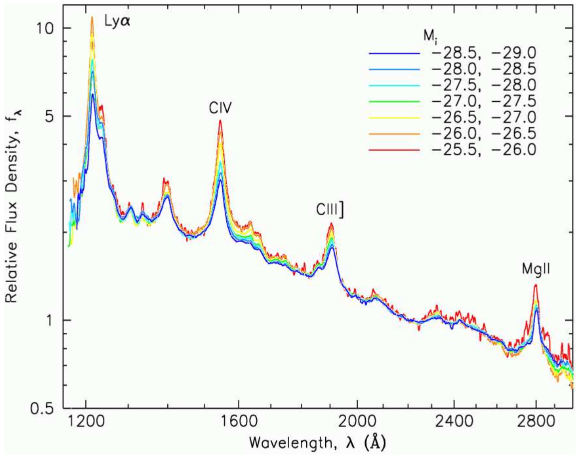

Average quasar spectra for $2.03 < z < 2.311$, normalized to the same flux at $\lambda = 2200$Å (vanden Berk et al., 2004, Fig. 1)

Review: Peterson (2006)

- Overall, spectral *shape* is luminosity independent
- Baldwin effect: Emission lines (esp. Lyα and C IV 1549Å) weaker in more luminous objects, although shape similar.

This chapter: physics of region emitting the broad lines.

Properties

General properties of the BLR from observed spectrum:

- Emission lines from BLR: typical for $T \sim 10^4$ K (photoionization)
- Lines have widths of 500...25000 km s^{-1}

  Thermal motion:

  $$E_{\text{kin}} = \frac{1}{2} m_{\text{p}} v^2 = \frac{3}{2} kT \tag{8.1}$$

  $\Longrightarrow$ Typical thermal speed:

  $$v \sim \sqrt{\frac{3kT}{m_{\text{p}}}} \sim 20\,\text{km}\,\text{s}^{-1} \tag{8.2}$$

- Line broadening is due to supersonic bulk motion of BLR emitting gas
- No [O III] 4959/5007 lines $\Longrightarrow n \gtrsim n_{\text{crit, 5077}} \sim 10^8\,\text{cm}^{-3}$.
- C iii] 1909 line sometimes broad, so $n \lesssim n_{\text{crit, 1909}} \sim 10^{10}\,\text{cm}^{-3}$.

  More detailed analyses show C iii] to originate in region different from Lyα emitting region, typical densities can be as high as $10^{11}\,\text{cm}^{-3}$.

Location

Location of BLR from line width:

Assume emitting gas on a circular orbit:

Kepler speed:

$$\frac{mv^2}{r} = \frac{GMm}{r^2} \quad \Longrightarrow \quad v = \sqrt{\frac{GM}{r}} \tag{8.3}$$

such that

$$r = \frac{GM}{v^2} = 3600\,\mathrm{AU}\left(\frac{M}{10^6\,M_\odot}\right)\left(\frac{v}{500\,\mathrm{km\,s^{-1}}}\right)^{-2} \tag{8.4}$$

The BLR is located close to the central black hole.

Note: BLR probably does *not* consist of gas on circular orbits around the BH, so real size is larger.

BLR: Mass

Mass determination: Determine number of emitting atoms from line strength, e.g., Hβ (less influenced by radiative transfer effects than Lyman lines)

Line emissivity:

$$j_{\mathrm{H}\beta} = n_\mathrm{e} n_\mathrm{p} \alpha_{\mathrm{H}\beta} \frac{h\nu_{\mathrm{H}\beta}}{4\pi} = n_\mathrm{e}^2 \alpha^{\mathrm{eff}}_{\mathrm{H}\beta} \frac{h\nu_{\mathrm{H}\beta}}{4\pi} = 1.24 \times 10^{-25}\,\mathrm{erg\,s^{-1}\,cm^{-3}\,sr^{-1}} \frac{n_\mathrm{e}^2}{4\pi} \tag{8.5}$$

where $\alpha^{\mathrm{eff}}_{\mathrm{H}\beta}$: effective recombination coefficient for $n = 4 \rightarrow n = 2$ transition (weakly temperature dependent).

Total Hβ luminosity:

$$L_{\mathrm{H}\beta} = \iint j_{\mathrm{H}\beta}\,\mathrm{d}\Omega\,\mathrm{d}V = \frac{4\pi n_\mathrm{e}^2}{3} \cdot 1.24 \times 10^{-25} r^3 f\,\mathrm{erg\,s^{-1}} \propto \int n_\mathrm{e}^2 \mathrm{d}V \tag{8.6}$$

where $\int n_\mathrm{e}^2 \mathrm{d}V$: emission measure, and f: filling factor.

BLR lines give BLR mass of $\sim 1\,M_\odot$ and $f \sim 10^{-3}$.

Observed lines are bright because of n^2-proportionality and high density of BLR gas.

BLR Line Variability, I

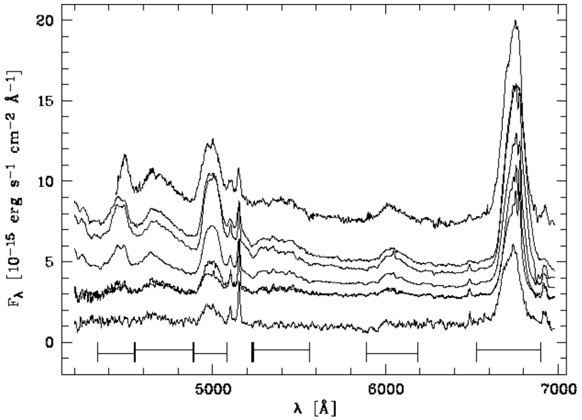

Spectral variability of NGC 7603 (Sy 1), top to bottom: Dec 98, Dec 93, Sep 93, Aug 92, Jul 90, Oct 88, and Oct 79 (Kollatschny, Bischoff & Dietrich, 2000, Fig. 2)

Broad lines are variable on timescales from days to years.

BLR Line Variability, II

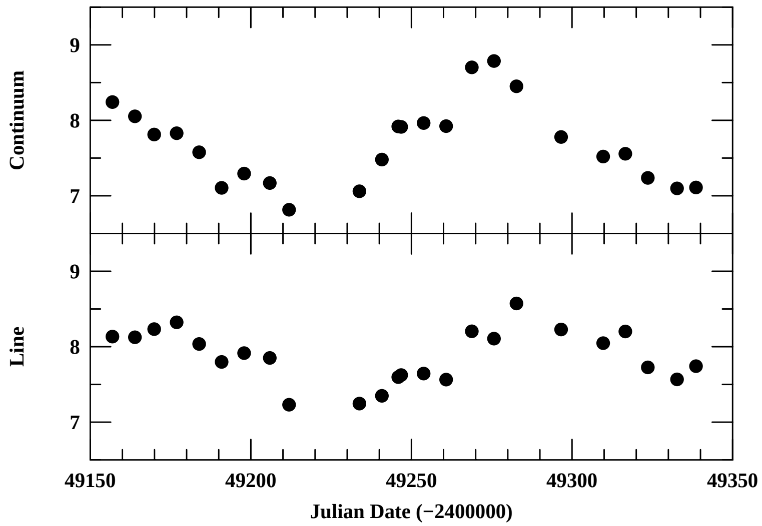

Continuum and Hβ fluxes for Mkn 335 (Peterson, 2001, Fig. 23)

BLR Line Variability, III

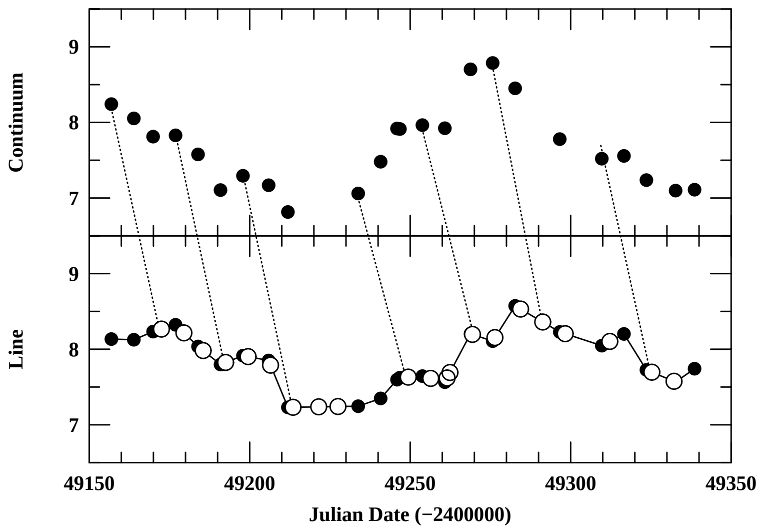

Mkn 335: Hβ line lags continuum by 15.6 d (Peterson, 2001, Fig. 24)

Reverberation Mapping

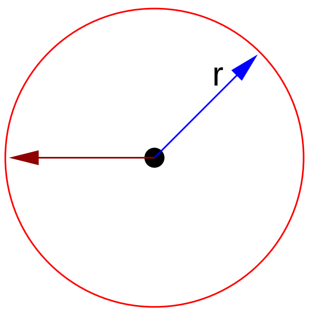

AGN time variability helps to map gas around Black Hole.

Flash at time $t = 0$ will illuminate gas at distance r after time delay

$$\tau = r/c \tag{8.7}$$

Gas is ionized by flash. Recombination timescale of gas is

$$\tilde{\tau} = \frac{1}{n_e \alpha} \sim 40 n_{11}^{-1}\,\mathrm{s} \tag{8.8}$$

i.e., “quasi instantaneous”.

Reverberation Mapping

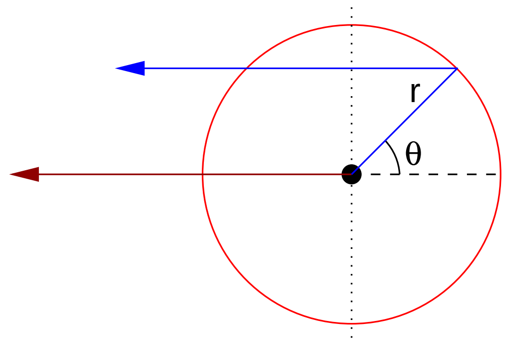

Light emitted by illuminated gas will be observed only after a time delay.

Extra distance traveled by light from r:

$$r' = r + r\cos\theta \tag{8.9}$$

Time delay due to light travel effect:

$$\tau = (1 + \cos\theta)\frac{r}{c} \tag{8.10}$$

Reverberation Mapping

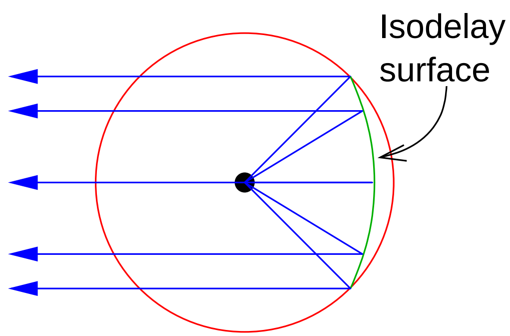

Time delay was given by:

$$\tau = (1 + \cos\theta)\frac{r}{c} \tag{8.10}$$

Locus of points with same time delay (isodelay surface):

$$r(\tau) = \frac{c\tau}{1 + \cos\theta} \tag{8.11}$$

(i.e., a parabola)

Reverberation Mapping

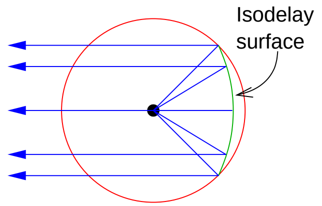

Assume that line intensity increases by factor ζ when BLR gas is illuminated by flash.

$\Longrightarrow$ total line emissivity increase from the isodelay surface:

$$\Psi(\theta)d\theta = \zeta \cdot 2\pi r^2 \sin\theta d\theta \qquad (8.12)$$

This assumes that conditions in BLR at r are the same everywhere.

$\Psi(r)d\theta$ corresponds to a response at time delay τ:

$$\Psi(\tau)d\tau = \Psi(\theta)d\theta \left|\frac{d\theta}{d\tau}\right| d\tau = \zeta \cdot 2\pi r^2 \sin\theta \cdot \frac{c}{r\sin\theta} d\tau = 2\pi\zeta r c d\tau \qquad (8.13)$$

where $\tau = (1+\cos\theta)r/c$, i.e., $d\tau/d\theta = -\sin\theta \cdot r/c$ was used.

Reverberation Mapping

In reality, AGN does not emit shots, but nucleus varies stochastically $\Longrightarrow$ **Reverberation mapping** (Blandford & McKee, 1982)

Describe continuum variability as $C(t)$.

Observed line variability, L, is:

$$L(t) = \int_{-\infty}^{+\infty} \Psi(\tau)C(t-\tau)d\tau \qquad (8.14)$$

(“convolution” of C with kernel $\Psi(\tau)$).

Observational problem is the inverse of Eq. (8.14): Given $L(t)$, determine $\Psi(\tau)$.

($C(t-\tau)$ is known from continuum variations), provided the lightcurve is long enough, as τ can be days to months!

Reverberation Mapping

To solve equations such as

$$L(t) = \int_{-\infty}^{+\infty} \Psi(\tau)C(t-\tau)d\tau \qquad (8.14)$$

for Ψ, the standard approach in mathematics is to determine the Fourier transform of $L(t)$:

$$L(f) = \int_{-\infty}^{+\infty} L(t)e^{-2\pi i f t}dt \qquad (8.15)$$

inserting Eq. (8.14) gives

$$= \int_{-\infty}^{+\infty}\int_{-\infty}^{+\infty} \Psi(\tau)C(t-\tau)e^{-2\pi i f t}d\tau dt \qquad (8.16)$$

change order of integration

$$= \int_{-\infty}^{+\infty} \Psi(\tau) \int_{-\infty}^{+\infty} C(t-\tau)e^{-2\pi i f t}dt d\tau \qquad (8.17)$$

substitute $t-\tau \longrightarrow t'$

$$= \int_{-\infty}^{+\infty} \Psi(\tau) \int_{-\infty}^{+\infty} C(t')e^{-2\pi i f (t'+\tau)}dt' d\tau \qquad (8.18)$$

Reverberation Mapping

Therefore

$$L(f) = \int_{-\infty}^{+\infty} \Psi(\tau) \int_{-\infty}^{+\infty} C(t')e^{-2\pi i f (t'+\tau)}dt' d\tau \qquad (8.18)$$

move constant outside of the inner integral and drop the prime

$$= \int_{-\infty}^{+\infty} \Psi(\tau)e^{-2\pi i f \tau} \int_{-\infty}^{+\infty} C(t)e^{-2\pi i f t}dt d\tau \qquad (8.19)$$

since the inner integral is a constant this gives

$$= \int_{-\infty}^{+\infty} e^{-2\pi i f \tau}\Psi(\tau)d\tau \cdot \int_{-\infty}^{+\infty} C(t)e^{-2\pi i f t}dt \qquad (8.20)$$

which is the product of the Fourier transforms of C and Ψ:

$$L(f) = \Psi(f) \cdot C(f) \qquad (8.21)$$

The Fourier transform of L is the product of the Fourier transforms of Ψ and C.

This is just the **convolution theorem** of Fourier theory.

Reverberation Mapping

Blandford & McKee (1982): Since $L(f)$ and $C(f)$ can be measured, we can determine $\Psi(f)$ and then do an inverse FT:

$$\Psi(t) = \frac{1}{2\pi}\int_{-\infty}^{+\infty} \Psi(f) e^{+2\pi i f t} df \qquad (8.22)$$

so we can in principle measure $\Psi(f)$.

In practice: Fourier approach does not work.

Reason: Sparse sampling of lightcurves

$\Longrightarrow$ Potential of reverberation mapping has not yet been realized!

What *is* possible is to determine size of BLR from reverberation mapping

Reverberation Mapping

To get BLR size from reverberation, work in time domain and determine cross correlation of $L(t)$ and $C(t)$:

$$\text{CCF}(\tau) = \int_{-\infty}^{+\infty} L(t)C(t-\tau)dt \qquad (8.23)$$

insert $L(t)$ from Eq. (8.14):

$$= \int_{-\infty}^{+\infty} C(t-\tau) \int_{-\infty}^{+\infty} C(t-\tau')\Psi(\tau')d\tau'\,dt \qquad (8.24)$$

change order of integration

$$= \int_{-\infty}^{+\infty} \Psi(\tau') \int_{-\infty}^{+\infty} C(t-\tau)C(t-\tau')dt\,d\tau' \qquad (8.25)$$

and introduce the auto correlation function, ACF,

$$= \int_{-\infty}^{+\infty} \Psi(\tau')\text{ACF}(\tau-\tau')d\tau' \qquad (8.26)$$

where

$$\text{ACF}(\tau) = \int_{-\infty}^{+\infty} C(t)C(t-\tau)dt \qquad (8.27)$$

Reverberation Mapping

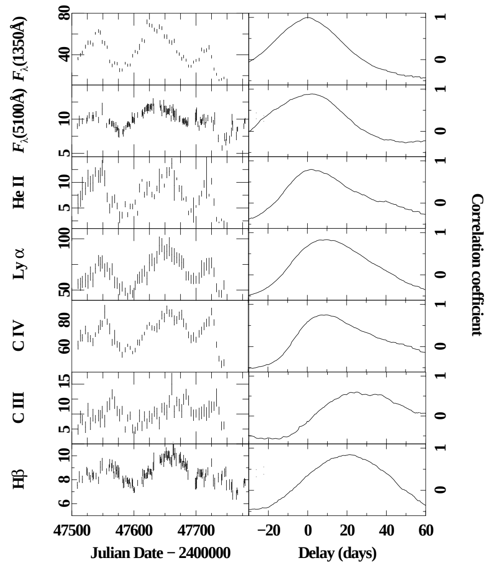

CCF has a peak at the lag for which $C(t)$ and $L(t)$ match best

$\Longrightarrow$ Based on the CCF we can measure the size of the BLR.

In practice, one has to interpolate $C(t)$ and $L(t)$ to determine CCF using a discretized version of the integrals shown previously.

Light curves and CCFs with respect to 1350Å UV continuum for NGC 5548 (Clavel et al., 1992; Peterson, 2001).

Reverberation Mapping

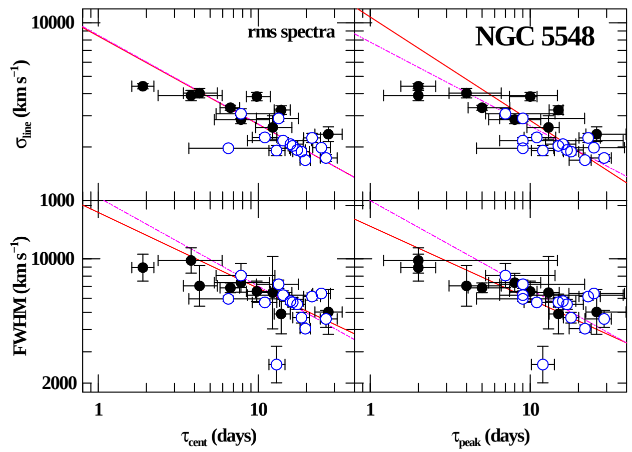

(Peterson et al., 2004, Fig. 3)

As expected: broadest lines vary fastest.

Also found: higher ionization lines vary fastest $\Longrightarrow$ BLR has stratified ionization structure